RSC Advances

ROYAL SOCIETY OF CHEMISTRY

www.rsc.org/advances

Tuning the mechanical and morphological properties of self-assembled peptide hydrogels via control over the gelation mechanism through regulation of ionic strength and the rate of pH change

Rui Li[ac*], Conor C. Horgan[b*], Benjamin Long[a], Alexandra L. Rodriguez[b], Lauren Mather[a], Colin J. Barrow[a], David R. Nisbet[b*] and Richard J. Williams[a*]

Hydrogels formed by the self-assembly of peptides are promising biomaterials. The bioactive and biocompatible molecule Fmoc-FRGDF has been shown to be an efficient hydrogelator *via* a π-β self-assembly mechanism. Herein, we show that the mechanical properties and morphology of Fmoc-FRGDF hydrogels can be effectively and easily manipulated by tuning both the final ionic strength and the rate of pH change. The increase of ionic strength, and consequent increase in rate of gelation and stiffness, does not interfere with the underlying π-β assembly of this Fmoc-protected peptide. However, by tuning the changing rate of the system's pH through the use of glucono-δ-lactone to form a hydrogel, as opposed to the previously reported HCl methodology, the morphology (nano- and microscale) of the scaffold can be manipulated.

Introduction

During the last three decades, biomaterials have been widely used as scaffolds to provide the essential physical, chemical and biological support required to regenerate damaged endogenous cells and to promote the survival and/or differentiation of exogenously transplanted cells.[1] The utilisation of self-assembly for the engineering of functional biomaterials is a promising research area with great potential for the treatment of injury or disease.[1] Recently, focus has been given to self-assembling peptides (SAPs) as they can form supramolecular structures which concomitantly present biochemical and physicochemical cues to control cell behaviour, including adhesion or differentiation[2,3]. For example, the biologically active epitope, arginine-glycine-aspartate (RGD), has been incorporated into SAPs and was shown to interact

with cells *in vitro*, influencing cell behaviour such as adhesion and viability.[4-6]. Furthermore, as they are formed of peptides, they are physiologically relevant and can be easily biodegraded *in vivo* to benign by-products.[1] As such, the nano- and micro-structured assembly of a promising class of SAPs incorporating the 9-fluorenylmethoxycarbonyl (Fmoc) group has been studied by us and others for use as biomaterials.[7,8,9-14]

Mechanical properties of the extracellular matrix (ECM) are related to various biological processes including cell proliferation, differentiation, migration, and collective cell behaviour.[15] Hence, the control of mechanical and morphological properties of SAP hydrogels is necessary in order to closely mimic the native ECM both for *in vitro*[16] and *in vivo*[17] applications. Two effective approaches to trigger hydrogelation of SAPs and regulate the mechanical properties of hydrogels are through control of pH and ionic strength.[18,19] Due to the zwitterionic nature of peptides, pH switch methodology has been widely used to induce hydrogelation.[5,7,20] The pH switch method is a facile route for hydrogel formation, but gelation can occur too rapidly leading to the formation of inhomogeneous, turbid hydrogels. Adams, *et al.* found that using glucono-δ-lactone (GdL) as the acidic component of a pH switch could slowly and controllably trigger formation of homogeneous and transparent hydrogels.[21] In Adams' study, gels formed using GdL were homogeneous and had much higher elastic (G') and viscous (G'') moduli compared to those formed using hydrochloric acid (HCl). However, these mechanical properties described are contradictory to many previous observations; in general, an increase in the rate of gelation is proportional to an increase in the final stiffness of the hydrogel[22,23]. In addition, previous research has shown that by altering the ionic strength of a system, the G' of a hydrogel can be controlled. Huang *et al.,* amongst others, have shown that the mechanical properties of hydrogels can be significantly improved

by the addition of salts;[19,22,24] also indicating that the rate of gel formation is linked to ionic strength.[24]

Previously, we have demonstrated that the designed SAP, Fmoc-FRGDF, is an effective material both *in vivo*[14] and *in vitro*[25]. Using this molecule as a platform, we demonstrate the control over the biologically relevant hydrogels using a pH switch methodology with varying ionic strength and acidic components: 0.05 M phosphate buffered saline (PBS) using GdL compared with 0.05 M PBS using HCl as potential cell culture platforms due to physiologically relevant final conditions. We explore the use of increased ionic strength to control the stiffness of the final hydrogels by controlling the ionic strength with 0.25 M, 0.5 M and 0.75 M PBS, allowing their potential use for environmentally responsive hydrogels[26, 27], drug delivery[28], and biosensing[29]

Results and discussion

Peptide self-assembly

In order to improve the versatility of our previously reported SAP hydrogelator, Fmoc-FRGDF, we sought to investigate the mechanical and morphological properties of the hydrogel formed under variation of ionic strength, using PBS, and pH change speed through the use of GdL. Such control over mechanical and morphological properties of Fmoc-FRGDF would extend the scope of SAPs for *in vivo* and *in vitro* applications,

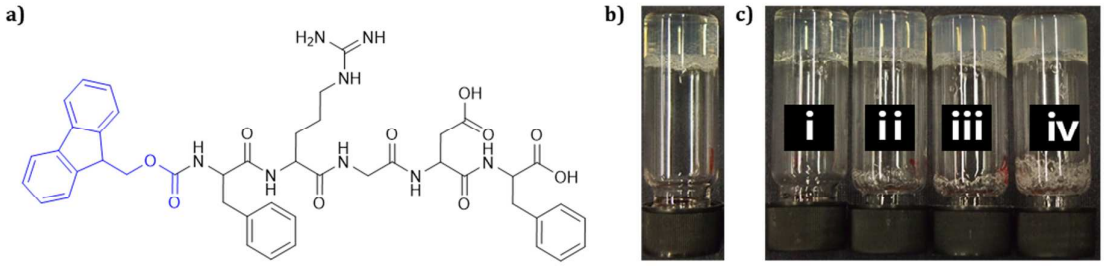

Fig.1 a) The chemical structure of Fmoc-FRGDF (Fmoc group highlighted in blue). (b) Hydrogel formed using GdL in 0.05 M PBS and (c) Using HCl at different PBS concentration i) 0.05 M PBS, ii) 0.25 M PBS, iii)0.5 M PBS, and iv) 0.75 M PBS.

In the current study, Fmoc-FRGDF was synthesised by traditional Fmoc-protected solid phase peptide synthesis (SPPS) methodology and a white crystalline powder was produced at high purity (>95%) (Fig. 1).

Firstly, in order to identify the correct concentration of GdL needed to equilibrate the SAP hydrogel at pH 7.4, a series of timescale experiments were conducted (Fig. 2a). A minimal volume of dilute Sodium hydroxide (NaOH) was added to the system in order to totally dissolve the peptide/water mixture, into which crystalline GdL was mixed. It was shown that the pH of the system equilibrated over a period greater than 8 hours, due to slow hydrolysis of GdL,[21] and it was noted that 0.16% (w/v) provided a sample with the desired pH of 7.4. All samples were unable to form stable gels without the addition of PBS. When applied to our target SAP sample containing PBS, 0.16% (w/v) GdL with 0.05 M PBS, a clear stable hydrogel that passed the inversion test was formed within 120 minutes. The formation of a stable gel with PBS using GdL shows the effect of ionic strength on the gelation.

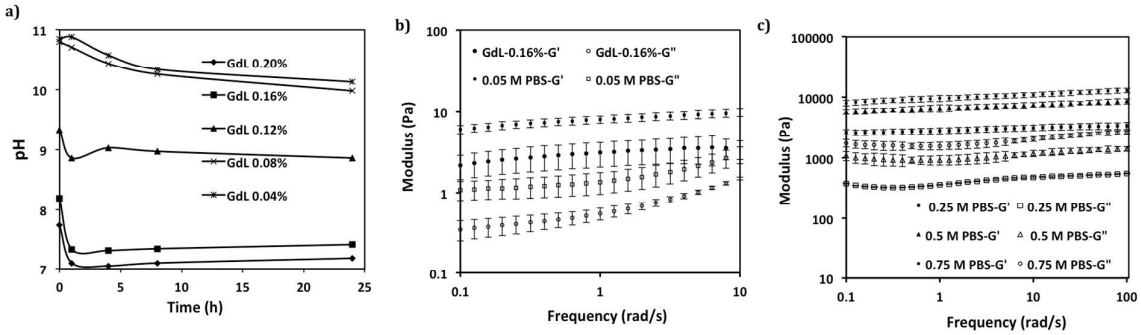

Fig. 2 a) The pH change over time when GdL is added to Fmoc-FRGDF. b) Dynamic moduli G' and G" of hydrogels formed using 0.16 % GdL in 0.05 M PBS and using HCl at 0.05 M PBS and c) using HCl at different concentration of PBS (0.25 M, 0.5 M, 0.75M).

The remaining gel samples were produced by a well-established pH switch methodology,[7] where dilute NaOH was used to solubilise the peptide/water mixture, and HCl was then added drop wise to lower the systems pH. Once the pH was reduced to 7.4, different concentrations of PBS were subsequently added in order to stabilise the pH of the hydrogels. When using HCl, the decrease in pH was instantaneous, relative to the GdL method, but required constant mixing in order to maintain a uniform pH profile. At the lowest PBS concentration (0.05 M) the peptide formed a clear hydrogel, which passed the inversion test within 120 minutes. At a higher PBS concentration of 0.25 M the SAP formed clear hydrogel within 30 minutes. At much higher concentrations of PBS, 0.5 M and 0.75 M, the hydrogel was formed within 5 and 2 minutes, respectively. The same phenomenon was reported when DMEM media was used to form hydrogels using a Fmoc-FF/Fmoc-RGD mixture, where counter-ions screen charged residues decreasing molecular repulsion.[5] However, the clarity of hydrogels decreased at 0.5 M PBS and became opaque at 0.75 M PBS (Fig. 1b). It is possible that this opaque character was due to the increased hydrophobic interactions promoted at higher ionic strength, boosting both the co-assembly of the peptides as well as possible non-specific aggregation through the "salting out" effect, leading to a cloudy gel.[30] However, Feng et al. noted the opposite trend where their hydrogels became transparent with an increase in ionic strength, suggesting that this effect is gelator specific.[30]

Determination of mechanical properties

With a range of hydrogels now in hand, the gels were characterised mechanically, spectroscopically and visually in order to elucidate the effects of both gelation rate and ionic strength on their structures and properties. The mechanical properties of the hydrogels were measured and compared using parallel-plate rheological analysis (Fig. 2b & c). The analysis showed that the G', at low frequencies (≤ 10 rad/s), of the hydrogel

formed using GdL and 0.05 M PBS was lower (G' ~ 3.5 Pa, 10 rad/s) than that of the hydrogel formed using HCl and 0.05 M PBS (G' ~ 10 Pa, 10 rad/s). At higher sweep frequencies (> 10 rad/s), the G' and G" of the hydrogel formed by GdL crossed (at 20 rad/s), which indicates gel-sol transition, characteristic of poor mechanical stability. In contrast, for all gels formed using HCl, the elastic moduli were dominant over the viscous moduli at all frequencies tested, indicating that gel structure was retained throughout the experiment.

The rheometry data also indicated a change in stiffness in relation to ionic strength. In Fig. 2c we can see that an increase in PBS concentration from 0.05 M to 0.75 M was accompanied by a G' increase of several orders of magnitude when using HCl to tune the pH. As indicated earlier, at a PBS concentration of 0.05 M, the gel G' was small (~ 10 Pa, 10 rad/s), when the PBS concentration was increased to 0.25 M, the G' increased by two orders of magnitude (~ 3200 Pa, 10 rad/s). At much higher PBS concentrations, 0.5 M and 0.75 M PBS, G' (~ 7500 Pa and ~ 11000 Pa at 10 rad/s, respectively) values were also larger by several orders of magnitude in comparison to the gel formed at a concentration of 0.05 M PBS. The stiffness enhancement may be due to faster gel formation rates, which have been shown to lead to stiffer hydrogels[19,22,23,30] and stabilisation of hydrophobic interactions through the "salting out" effect.[27] Furthermore, for all PBS concentrations, the G' values are essentially independent of the frequency in the tested range, the elastic moduli were much higher than viscous moduli (~ 500 Pa, ~ 1200 Pa and ~ 2000 Pa of 0.25, 0.5 and 0.75 M PBS at 10 rad/s, respectively). Additionally, there was no crossover point between G' and G", which indicates a stable fibrillar network.[19]

Confirmation of self-assembly mechanism

As the stiffness was increased by several orders of magnitude, and the gel became opaque at higher PBS concentrations, we needed to verify if the supramolecular structures were still driven by a π-β assembly. To confirm the assembly mode, Fourier transform infrared spectroscopy (FT-IR) and circular dichroism (CD) were used to investigate the peptide secondary structure, and fluorescence spectroscopy was used to probe the environment of the Fmoc group. Using FT-IR, the amide I region is the most widely used region to assess peptide secondary structure.[31] As shown in Fig. 3a, all hydrogels have a characteristic strong IR absorbance peak at 1630 cm^{-1} and a shoulder at 1690 cm^{-1}, which indicates that anti-parallel β-sheet structure is dominant in all samples.[32] However, when the PBS concentration was raised above 0.5 M, there was an increased absorbance at ~1670 cm^{-1} which indicates partial random coil character (the wavelength had blue shift in this case).[5] The appearance of the less ordered random coil structure may also contribute to the opacity of the hydrogels through increased scattering. The dominant anti-parallel β-sheet secondary structure is in agreement with previous work on this class of material.[7,8,33,34] CD spectroscopic analysis was then used to confirm the secondary structure of the hydrogel. As shown in Fig. 3b, the Cotton effect at ~220 nm induced by n-π* transition provides further evidence for the formation of anti-parallel β-sheet structure,[35] confirming the results noted in the FT-IR. Another transition at around 260 nm is attributed to the bundling between fibers, analogous to the interactions between macromolecules.[6,8,34] Furthermore, while the shape and peak position in the spectra were retained in all samples which used HCl and varying concentrations of PBS, both the transition at 220 nm and 260 nm increased with the increase of PBS concentration when ≤ 0.5 M PBS were used. In contrast, at the highest PBS concentration, 0.75 M, these values decreased; this was either due to the opaque characteristic of the hydrogel at 0.75 M PBS or an increase in non-specific aggregation of

peptides at the higher ionic strength. The increase of magnitude of CD ellipticity shows that self-assembly of the peptides and bundling of fibrils is favored with a small increase of ionic strength, but fibril formation is possibly disrupted if the ionic strength is raised too high. When using GdL to form the hydrogel, the overall shape of the spectra is different, the transition at 220 nm is comparable to that of 0.05 M PBS, indicating an anti-parallel β-sheet structure, but the peak at 260 nm is both larger in magnitude to that of 0.05 M PBS and the maximum is slightly shifted towards a higher energy. This shift in energy maximum may be due to a different bundling mechanism as a result of the slow rate of change in pH.

Fluorescence spectroscopy was used to monitor the environment of the fluorenyl group in order to monitor the effect of ionic strength on π-stacking interactions. The emission maximum wavelength of Fmoc-FRGDF in water (solution) is at 320 nm (Supp. Fig. 1), when a hydrogel of Fmoc-FRGDF is formed the emission peak is centred at 325 nm (Fig. 3c). The red shift is consistent with excimer formation and π-stacking of fluorenyl rings, as observed in similar systems.[5,7,36,37] The intensity of the peaks at 325 nm decreased with the increase of PBS concentration, due to the increasingly opaque hydrogels.

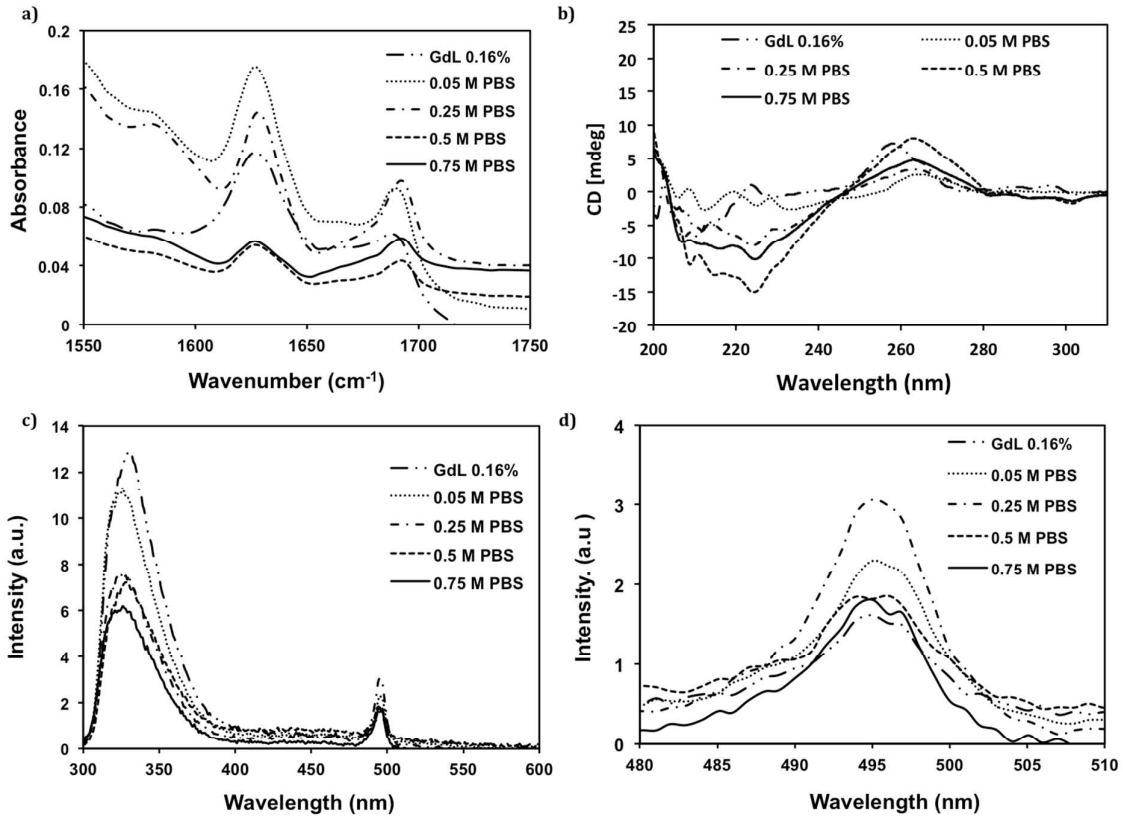

Fig. 3 Spectroscopic data for Fmoc-FRGDF hydrogels formed using 0.16 % GdL in 0.05 M PBS and using HCl and different concentration of PBS (0.05 M, 0.25 M, 0.5 M and 0.75 M). a) Truncated FT-IR spectra of amide I region; b) CD spectra; c) fluorescence spectra and d) enlargement of fluoroescence spectra in the region of 480-510 nm (J-aggregate).

A second emission peak centred at 495 nm was indicative of J-Aggregates.[5,6,7,33] The intensity of the emission from the hydrogel formed using GdL was the weakest. Furthermore, J-aggregate emission increased with the increase in PBS concentration from 0.05 M to 0.25 M PBS, which, conversely, was suppressed at PBS concentrations 0.5 M to 0.75 M — the opaque nature likely affected the emission. These results again support the CD and FT-IR data, in which the "salting out" effect played a role in fibril formation.

Investigation of nano- and micro- morphology

As spectroscopy confirmed that the π-β assembly was undisturbed by changes in ionic strength, both TEM and AFM were used to assess the nano and micro morphology of the fibres. TEM imaging was used to visualise the hydrogel nanostructure. For the hydrogel formed by GdL, the single fiber diameter was < 5 nm; and for those formed by HCl solution at different PBS concentration, the nanofibrils' diameter were all > 5 nm (Fig.4). The formation of thinner fibrils for GdL may be due to the moderate change of the system's pH. Well-ordered fibrillar networks were formed using GdL and PBS concentration ≤ 0.5 M. At PBS concentration 0.75 M, the networks were disordered with amorphous regions (Fig. 4e). The disorder of fibrils in comparison to the other examples helps to explain the opaque characteristic and decreased order noted in the spectroscopic data. The faster assembly speeds lead to a highly entangled structure but also favor a disordered assembly. The increased entanglement was the likely cause for the rise in hydrogel stiffness noted in the rheometry. Interestingly, thicker bundles formed by the nanofibrils when using GdL, as generally noted by this class of gelators at similar GdL concentration,[38] and the tubular morphology of the fibre was maintained when formed using GdL, but the bundling and flexibility of the fibrils was altered, becoming more 'ribbon like'.

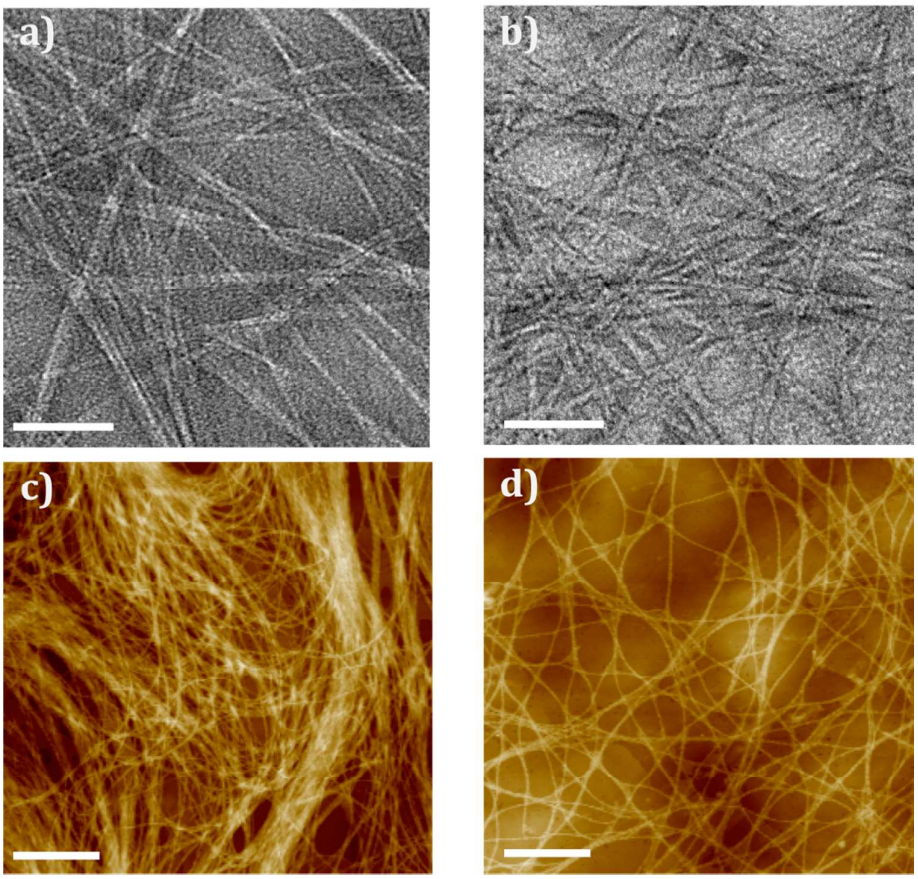

Fig. 4 Nano and microstructure of Fmoc-FRGDF hydrogels (top panel TEM and bottom panel AFM). a), c) formed using 0.16 % GdL in and b), d) dropwise HCl .(scale bar represents 50 nm AFM 1 µm)

AFM images (Fig. 4) revealed the entangled networks that underpin the hydrogels. A different morphology of the hydrogel formed using GdL was observed (Fig.4a); the nanofibrils were aligned in thick bundles, this reinforced the TEM result. The bundling may also be due to the moderate pH change of the hydrogel, and explains the shift in CD spectrum at 260 nm as the bundling morphology was significantly different from the entangled networks as shown in the other examples (Fig. 4b-e). As the ionic strength was increased using HCl at different PBS concentrations to form the hydrogel, the number of fibre entanglements and aggregates also increased. These entanglements and aggregates may be due to the increased random coil component disrupting the predominantly anti-parallel β-sheet structured nanofibrils, which could again be related to the increase in G' and opacity. It should be noted, however, that there was also an

increase in amorphous regions that could be responsible for the increase in opacity of the final gel.

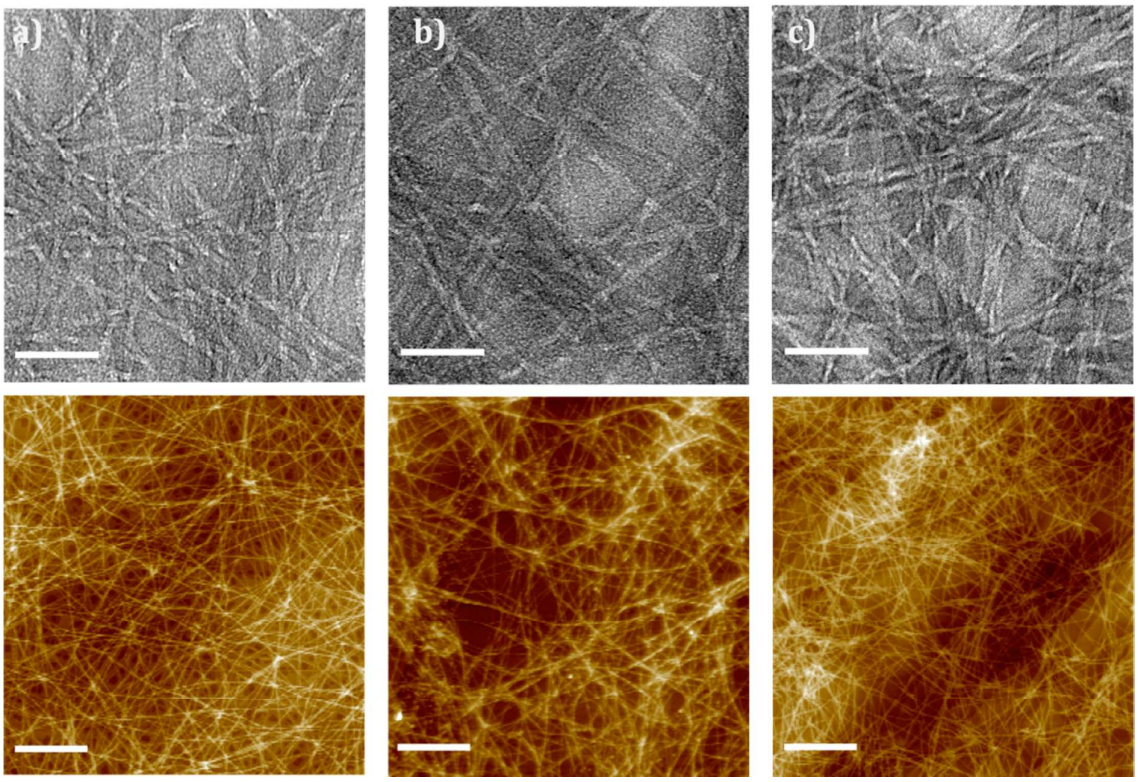

Fig. 5 Nano and microstructure of Fmoc-FRGDF hydrogels (top panel TEM and bottom panel AFM). formed using using HCL and a)) 0.25 M, b) 0.25 M and c) 0.75 M of PBS, respectively. (TEM scale bar represents 50 nm , AFM 1 µm).

Conclusions

In conclusion, GdL can be used in a slow pH switch methodology to form a clear hydrogel of Fmoc-FRGDF in a controlled fashion. Using GdL it was possible to form a microstructure where the nanofibrils were aligned with relatively few entanglements, resulting in a weaker gel. Control of PBS concentration in conjunction with an HCl based pH switch methodology can be used to efficiently tune the mechanical properties of hydrogels without altering their anti-parallel β-sheet structure and π-β assembly. The stiffness of hydrogels was increased by several orders of magnitude by increasing PBS concentration. The differences in stiffness were attributed to a faster rate of gel

formation leading to a network of smaller highly entangled fibres. The increase in stiffness was accompanied with a decrease in gel clarity, which is of concern for applications requiring optical visualisation of the interior of the gel. Such control over gel properties will provide an effective method to imitate the different native ECM structures *in vitro* and tuning of hydrogels for three-dimensional cell cultures and *in vivo*, as well as a range of mechanical properties for of biomaterial applications.

Experimental

Peptide synthesis

The synthesis of Fmoc-FRGDF was performed as previously reported.[6] Purity of Fmoc-FRGDF was > 95% as determined by reverse phase high performance liquid chromatography.

GdL acidified hydrogel formation

10 mg of crystalline Fmoc-FRGDF was added to a 4 mL glass vial. 285 µL Mili-Q water (purified by Mili-Q Advantage A10 System, Merck Milipore, Australia) and 65 µL sodium hydroxide (NaOH) 0.5 M solution were added and the vial vortexed until the peptide was dissolved. 160 µL of 10 mg/mL GdL solution was then added and finally, 490 µL 0.1 M PBS solution (pH 7.4) was added to stabilise the pH. The resulting solution was kept at room temperature for gelation (total peptide concentration 1 wt%).

HCl Acidified hydrogel formation

10 mg of crystalline Fmoc-FRGDF was added to a 4 mL glass vial. 400 µL Mili-Q water and 65 µL NaOH 0.5 M solution were added and vortexed until dissolved. The solution was then neutralised to pH 7.4 *via* drop wise addition of 0.1 M HCl (Asia Pacific Specialty Chemicals Ltd., Australia) with vortexing. Finally, PBS (pH 7.4, 0.1 M, 0.5 M, 1.0 M and 1.5 M) was added into the solution to make the total volume to 1 mL and the resulting solution kept at room temperature for gelation (total peptide concentration 1 wt%).

GdL titration

5 mg of crystalline Fmoc-FRGDF was added to a 4 mL glass vial. For the pH–time analysis of hydrogel formed by GdL method, 50 µL Mili-Q water (purified by Mili-Q Advantage A10 System, Merck Milipore, Australia) and 25 µL of 0.5 M NaOH were added by vortexing until the peptide was totally dissolved. 325-405 µL Mili-Q water was then added into the solution. Finally, 20-100 µL GdL solution (10 mg/mL) was added to make the total volume to 500 µL. The pH was then monitored over time (total peptide concentration 1 wt%).

Circular dichroism

Spectrum of hydrogels was measured using a Jasco J-815 circular dichroism spectrometer with the bandwidth 1 nm and integrations 2 s^{-1}. A 1 mm quartz cell (Starna Pty. Ltd., Australia) was used. Samples were prepared at a concentration of 0.05 wt% in order to achieve consistent loading and reduce scattering. The data were collected 3 times and average values were used for all the samples.

Fourier transform infrared spectroscopy

A Nicolet 6700 Fourier transform infrared spectroscopy (FT-IR) was used to collected spectra using attenuated total reflection (ATR) mode. 12 µL hydrogels were applied directly to the ATR crystal and scanned between the wavenumbers of 4000 and 400 cm^{-1} over 64 scans. A background scan of PBS buffer was applied before samples.

Fluorescence spectrophotometer

Fluorescence emission spectra were measured on a Cary Eclipse fluorescence spectrophotometer (Agilent Technologies, USA) with light measured orthogonally to the excitation light. The emission bandwidth was set at 5 nm. A scanning speed of 600 nm min^{-1} was used with a data pitch of 1 nm. Excitation wavelength was at 248 nm and emission data range between 300 nm and 600 nm. Quartz cuvette (Starna Pty. Ltd., Australia) of 1 mm path length were used for scanning. Samples were prepared at a concentration of 0.5 wt%.

Transmission electron microscopy

JEOL-2100 LaB6 transmission electron microscopy (TEM) (JEOL Ltd., Japan) at an operation voltage of 100 Kv was used for TEM images. Agar lacey carbon coated films on 300 mesh copper grids (Emgrid Pty. Ltd., Australia) were used as sample holder. For sample preparation, 12 µL of hydrogel was applied onto the grid and allowed it to absorb for 30 s, then using split Whatman filter paper (No.1) to wick off excess fluid. One drop of negative stain NanoVan (Bio-Scientific Pty. Ltd., USA) was put onto parafilm "M", then put the grid on the stain with carbon side down and allowed to stain for 5 min. Then, dried in air for 2 min with carbon side up, at last put the grids into grid box to leave it dry overnight.

Atom force microscopy

Atomic force microscopy (AFM) images of the samples were obtained using a Multimolde 8 (Bruker BioSciences Corporation, USA). The tips used were ScanAsyst-air probes with silicon tip on nitride lever (Bruker BioSciences Corporation, USA). The AFM was operated in peak force QNM. Calibration of deflection sensitivity, spring constant and tip radius of probes was done before sample imaging. Scan size was at 10 µm. For sample preparation, hydrogels were diluted to peptide concentration at 0.05 wt%, and 15 µL of diluted samples were applied on highly ordered pyrolytic graphite (HOPG) substrates (SPI, USA), the redundant samples were absorbed by pipette.

Rheometry

A Discovery Hybrid Rheometers (TA Instruments, USA) was operated at constant stress with a strain of 2.83%. An amplitude sweep was performed and showed no variation in G' and G" up to a strain of 60%. Frequency sweeps were performed over a range between 0.1 and 100 rad/s. Temperature was maintained at 25 °C via the use of Peltier plate control. Soak time was 30 min. Hydrogels were performed on a cone-plate geometry (40 mm, 2 º 1' 37") with a gap of 51 µm. A water trap was used to minimise evaporation.

Acknowledgements

This work was funded by an Australian Research Council Discovery Project (DP130103131). DRN was supported by an NHMRC Career Development Fellowship (APP1050684). RJW was supported by an Alfred Deakin Research Fellowship. The authors wish to thank Motilal Mathesh Shanmugam for assistance with AFM, Tao Zhang, and Ping'an Song for assistance with rheometry, San Seint Seint Aye for assistance with the synthesis of Fmoc-FRGDF.

Notes and references

[a] *Centre for Chemistry and Biotechnology, School of Life and Environmental Sciences, Deakin University, Waurn Ponds, VIC 3216, Australia,;*

[b] *Research School of Engineering, The Australian National University, Canberra,2601, Australia.*

[c] *Coconut Research Institute of Chinese Academy of Tropical Agricultural Sciences, Wenchang 571339, Hainan, China*

d School of Aerospace, Mechanical and Manufacturing Engineering, RMIT University, Bundoora, VIC, 3083 Australia. Phone: + 61 3 9925 6642, Email: richard.williams@RMIT.edu.au

**Indicates joint authorship*

References

1. N. Stephanopoulos, J. H. Ortony and S. I. Stupp, *Acta Materialia*, 2013, **61**, 912-930.
2. C. J. Newcomb, S. Sur, J. H. Ortony, O.-S. Lee, J. B. Matson, J. Boekhoven, J. M. Yu, G. C. Schatz and S. I. Stupp, *Nature Communications*, 2014, **5**.
3. D. R. Nisbet and R. J. Williams, *Biointerphases*, 2012, **7**, 1-14.

4. A. R. Morales, C. O. Yanez, Y. Zhang, X. Wang, S. Biswas, T. Urakami, M. Komatsu and K. D. Belfield, *Biomaterials*, 2012, **33**, 8477-8485.
5. M. Zhou, A. M. Smith, A. K. Das, N. W. Hodson, R. F. Collins, R. V. Ulijn and J. E. Gough, *Biomaterials*, 2009, **30**, 2523-2530.
6. V. N. Modepalli, A. L. Rodriguez, R. Li, S. Pavuluri, K. R. Nicholas, C. J. Barrow, D. R. Nisbet and R. J. Williams, *Peptide Science*, 2014, **102**, 197-205.
7. A. M. Smith, R. J. Williams, C. Tang, P. Coppo, R. F. Collins, M. L. Turner, A. Saiani and R. V. Ulijn, *Advanced Materials*, 2008, **20**, 37-41.
8. R. J. Williams, T. E. Hall, V. Glattauer, J. White, P. J. Pasic, A. B. Sorensen, L. Waddington, K. M. McLean, P. D. Currie and P. G. Hartley, *Biomaterials*, 2011, **32**, 5304-5310.
9. S. Toledano, R. J. Williams, V. Jayawarna and R. V. Ulijn, *Journal Of The American Chemical Society*, 2006, **128**, 1070-1071.
10. J. D. Hartgerink, J. R. Granja, R. A. Milligan and M. R. Ghadiri, *J. Am. Chem. Soc.*, 1996, **118**, 43-50.
11. K. Kobayashi, J. R. Granja and M. R. Ghadiri, *Angewandte Chemie International Edition in English*, 1995, **34**, 95-98.
12. M. R. Ghadiri, J. R. Granja, R. A. Milligan, D. E. McRee and N. Khazanovich, *Nature*, 1993, **366**, 324-327.
13. M. Reches and E. Gazit, *Science*, 2003, **300**, 625-627.
14. A. L. Rodriguez, T. Y. Wang, K. F. Bruggeman, C. C. Horgan, R. Li, R. J. Williams, C. L. Parish and D. R. Nisbet, *Journal of Materials Chemistry B*, 2014.
15. A. J. Engler, S. Sen, H. L. Sweeney and D. E. Discher, *Cell*, 2006, **126**, 677-689.
16. S. Sur, C. J. Newcomb, M. J. Webber and S. I. Stupp, *Biomaterials*, 2013, **34**, 4749-4757.
17. K. Mi, G. Wang, Z. Liu, Z. Feng, B. Huang and X. Zhao, *Macromol Biosci*, 2009, **9**, 437-443.
18. C. Tang, A. M. Smith, R. F. Collins, R. V. Ulijn and A. Saiani, *Langmuir*, 2009, **25**, 9447-9453.
19. B. Ozbas, J. Kretsinger, K. Rajagopal, J. P. Schneider and D. J. Pochan, *Macromolecules*, 2004, **37**, 7331-7337.
20. S. Y. Qin, S. S. Xu, R. X. Zhuo and X. Z. Zhang, *Langmuir*, 2012, **28**, 2083-2090.
21. D. J. Adams, M. F. Butler, W. J. Frith, M. Kirkland, L. Mullen and P. Sanderson, *Soft Matter*, 2009, **5**, 1856-1862.
22. Z. Luo, Y. Yue, Y. Zhang, X. Yuan, J. Gong, L. Wang, B. He, Z. Liu, Y. Sun, J. Liu, M. Hu and J. Zheng, *Biomaterials*, 2013, **34**, 4902-4913.
23. Z. Yang, G. Liang, M. Ma, Y. Gao and B. Xu, *Small*, 2007, **3**, 558-562.
24. H. Huang, A. I. Herrera, Z. Luo, O. Prakash and X. S. Sun, *Biophysical Journal*, 2012, **103**, 979-988.
25. V. N. Modepalli, A. L. Rodriguez, R. Li, S. Pavuluri, K. R. Nicholas, C. J. Barrow, D. R. Nisbet and R. J. Williams, *Peptide Science*, 2014, **102**, 197-205.
26. Z. Hu, Y. Chen, C. Wang, Y. Zheng and Y. Li, *Nature*, 1998, **393**, 149-152.
27. K. K. Westbrook and H. J. Qi, *Journal of intelligent material systems and structures*, 2007.
28. Y. Qiu and K. Park, *Advanced drug delivery reviews*, 2001, **53**, 321-339.
29. J. H. Holtz and S. A. Asher, *Nature*, 1997, **389**, 829-832.
30. Y. Feng, M. Taraban and Y. B. Yu, *Soft Matter*, 2012, **8**, 11723-11731.
31. W. K. Surewicz, H. H. Mantsch and D. Chapman, *Biochemistry*, 1993, **32**, 389-394.
32. J. T. Pelton and L. R. McLean, *Analytical Biochemistry*, 2000, **277**, 167-176.
33. R. J. Williams, A. M. Smith, R. Collins, N. Hodson, A. K. Das and R. V. Ulijn, *Nat Nanotechnol*, 2009, **4**, 19-24.
34. A. R. Hirst, S. Roy, M. Arora, A. K. Das, N. Hodson, P. Murray, S. Marshall, N. Javid, J. Sefcik, J. Boekhoven, J. H. Esch, S. Santabarbara, N. T. Hunt and R. V. Ulijn, *Nature Chemistry*, 2010, **2**, 1089-1094.
35. S. M. Kelly, T. J. Jess and N. C. Price, *Biochim Biophys Acta*, 2005, **1751**, 119-139.
36. Z. Yang, H. Gu, Y. Zhang and L. Wang, *Chemical Communications*, 2004, **2004**, 208-209.

37. H. K. Kang, D. E. Kang, B. H. Boo, S. J. Yoo, J. K. Lee and E. C. Lim, *The Journal of Physical Chemistry A*, 2005, **109**, 6799-6804.
38. L. Chen, K. Morris, A. Laybourn, D. Elias, M. R. Hicks, A. Rodger, L. Serpell and D. J. Adams, *Langmuir*, 2010, **26**, 5232-5242.